Journal of Inorganic Biochemistry 203 (2020) 110927

Contents lists available at ScienceDirect

Journal of Inorganic Biochemistry

journal homepage: www.elsevier.com/locate/jinorgbio

Complex formation processes and metal ion catalyzed oxidation of model peptides related to the metal binding site of the human prion protein

Gizella Csire, Ildikó Turi, Imre Sóvágó, Eszter Kárpáti, Csilla Kállay*

Department of Inorganic and Analytical Chemistry, University of Debrecen, H-4032 Debrecen, Hungary

A B S T R A C T

Interaction of copper(II) and nickel(II) ions with the Ac-PHAAAGTHSMKHM-NH_2 tridecapeptide containing the His85, His96 and His111 binding sites of human prion protein has been studied by various techniques. pH-potentiometry, UV–Vis and circular dichroism spectroscopy were applied to study the stoichiometry, stability and structure of the copper(II) and nickel(II) complexes, while HPLC-MS and MS/MS were used for identifying the products of copper(II) catalyzed oxidation. The copper binding ability of shorter fragments, namely the nonapeptide Ac-PHAAAGTHS-NH_2 and pentapeptide Ac-PHAAA-NH_2 have also been studied. The tridecapeptide is able to bind three equivalent of copper(II) ion, since the histidine residues behave as independent metal binding sites. Nevertheless, the metal binding ability of histidine residue mimicking the octarepeat domain (His85) is decreased, while the other parts of the peptide mimicking the histidines outside the octarepeat domain bind the copper ions in comparable concentration. On the other hand, this peptide is able to coordinate only two equivalents of nickel ion on the domains outside the octarepeat region. Furthermore the His96 binding site is more effective for the nickel ions. Both histidine and methionine residues are sensitive for oxidation, the oxidation of these residues are proved, and in the case of the histidine residues follows the order His96 > His85 ≫ His111.

1. Introduction

The human cellular prion protein, denoted PrP^C consists of 231 amino acids. PrP^C can be divided into two distinct regions: a flexible N-terminal region that is essentially unstructured and a C-terminal region comprising three α-helical structures and two small anti-parallel β-sheet structures [1,2]. Prion diseases, also known as transmissible spongiform encephalopathies (TSE), are a family of fatal neurodegenerative disorders. They include scrapie in sheep and goats, bovine spongiform encephalopathy in cattle, chronic wasting disease in deer, elk and kuru, Creutzfeldt-Jakob disease, fatal familiar insomnia and Gerstmann-Straussler-Scheinker syndrome in humans [3,4]. Clinically these diseases are characterised by dementia and motor dysfunction, while neuropathologically by amyloid deposition (in the form of prion protein), spongiform changes in the brain and neuronal loss [5]. The conformational changes of the normal form of the protein (PrP^C) to the disease-related scrapie isoform (PrP^{Sc}) are considered to be responsible for these diseases [6]. More and more experimental evidence supports that metal ions, especially copper(II) may take part in the biochemical processes related to the normal function of prion protein and/or its conformational changes. As a consequence, the interaction between copper(II) ion and prion protein and its peptide fragments was widely studied. Several reports can be found about the binding affinity of metal ions to prion protein. The high copper(II) binding affinity is due to the imidazole side chains of histidine residues in the sequence, which are primary binding sites for metal ions. It is widely accepted that at least six histidyl residues of human prion protein can take part in copper binding. These include four histidines of the octarepeat (His61, His69, His77 and His85) and two histidines (His96 and His111) outside the octarepeat domain. It is suggested by G. Legname et al. that all copper-binding sites are important to preserve the functional conformation of Pr^{PC}. The ability of Pr^{PC} in binding copper is key for maintaining the protein function and preventing its conversion to the prion state. Indeed, minimal structural changes especially at a non-octarepaet copper-binding site, may be sufficient to alter Pr^{PC} conformation and function, which may modulate its propensity to prion conversion [7,8].

The octarepeat was first described as the primary copper(II) binding site of the natural protein, but our systematic studies on the peptide fragments of the protein revealed that the order of copper(II) binding affinity of the various histidyl sites is His111 > His96 > His(octarepeat) [9–12]. The enhanced thermodynamic stability of the copper(II) complexes with the fragments containing His111 or His96 residues can be easily explained by the difference in chelate ring sizes formed with histidines inside and outside the octarepeat domain. Histidines of the octarepeat fragments are preceded by proline which is break-point for amide deprotonation [13], and as a consequence amide coordination can only occur towards the C-terminus in the form of a seven-membered chelate [14–16]. The thermodynamic stability of the peptide complexes having this coordination mode is smaller than those formed with His96 and/or His111 in the form of six-membered chelates

* Corresponding author.
E-mail address: kallay.csilla@science.unideb.hu (C. Kállay).

https://doi.org/10.1016/j.jinorgbio.2019.110927
Received 12 August 2019; Received in revised form 23 October 2019; Accepted 12 November 2019
Available online 13 November 2019

[10–12,17]. The size of chelate rings and the coordinated donor atoms are the same for His96 and His111, but the stability constants are always higher for the copper(II)-peptide complexes containing His111 residues. However, this trend is just the opposite for the nickel(II) complexes [18]. Our studies also revealed that the sequence -GTHS-, which contains short side chains around His96, is better suited for the strict square planar coordination geometry of nickel(II) complexes apart from the position of this binding site in the studied peptides chain. On the other hand, the formation of 5-coordinated copper(II) species is usually more favored with the -MKHM- sequence, which contains longer side chains around His111 and therefore tends to coordinate axially, however the selectivity depends not only on the neighbouring amino acids but the distant amino acids also have an influencing role. These observations were reported by the studies of octapeptides containing both the MKHM and GTHS sites [19]. These studies are now completed by an N- and C-terminally protected tridecapeptide (Ac-PHAAAGTHSMKHM-NH_2), which also contains the main binding site of the octarepeat domain in addition to the above mentioned His96 and His111 moieties. The glycine amino acids of the octarepeat part are replaced by alanine because of the CD studies. Shorter fragments of the tridecapeptide (Ac-PHAAAGTHS-NH_2 and Ac-PHAAA-NH_2) were also studied to clarify the differences in the metal-binding ability of histidine residues at different positions in the prion protein.

In addition to the complex formation, copper ions play an important role in various oxidative reactions of peptides. It has an importance also in the case of prion protein. Copper-bound prion protein undergoes redox cycling in the presence of electron donors, such as superoxide ions, dopamine or ascorbate. The mechanism of oxidative damage to proteins involves catalysis by transition metals [20,21]. This process consists of reduction of Fe(III) or Cu(II) by electron donors, such as O_2^-, H_2O_2, ascorbate or thiols, and generation of the hydroxyl radical through reduction of H_2O_2 by the reduced metals. This highly reactive free radical immediately oxidizes neighbouring amino acid residues; The metal-catalyzed oxidation (MCO) of proteins is mainly a site-specific process in which only one or a few amino acids at the metal-binding sites of the protein are preferentially oxidized [22,23]. This reaction typically results in structural alterations and loss of enzyme activity [20,21].

Histidine and methionine are the most important targets of protein oxidation. 2-oxo-histidine was found to be the predominant product of MCO in histidine containing proteins such as human growth hormone [24] and human relaxin [25]. Other unidentified protein degradation products have been detected, including the formation of asparagine and/or aspartyl from histidyl residues [26,27] Met(O) (methionine sulfoxide) is proposed to be the major product of MCO of methionine [28]. Higher oxidized products of methionine may have an additional oxygen at the sulfur atom or at one of the carbon atoms, or addition of a perhydroxyl group (OOH) at the sulfur atom [29,30]. The oxidation of proteins may also lead to cleavage of peptide bonds.

However, in our last publication on this subject the following conclusions were drawn. The peptide which does not contain methionine does not undergo oxidation, only the fragmentation of the peptide chain is observed. The cleavage of the peptide bonds occurs far away from the histidine residue. On the other hand, in the case of methionine containing peptides, the peptide chain was not cleaved; the presence of methionine residues protected the peptides from fragmentation. In these cases copper(II) ions catalyzed the oxidation of methionine to methionine sulfoxide. This process occurred randomly, it did not depend on the position of the methionine; methionine residues undergo oxidation either involved in the coordination of the copper(II) ions, or near or far the binding sites. Our results revealed that methionine residues of prion protein can play a role as ROS scavenger [31].

The binding preference of the wild type prion protein is well-known from earlier studies. However these fragments contain several side chains which may have an effect on the complex formation processes even though they are far from the metal binding sites. Therefore in the continuation of this work we report the interaction of copper(II) and nickel(II) ions with the Ac-$PH^{85}AAAGTH^{96}SM^{109}KH^{111}M^{112}$-$NH_2$ including both coordination and oxidation. The binding sites are the same in this peptide, but this contains only amino acids in the direct environment of the bound metal ion. Although nickel ions have no biological relevance in the case of prion protein, they are also involved in this study. The coordination chemistry of copper(II) and nickel(II) ions are rather similar, therefore nickel(II) ions are commonly used models of the copper(II) – peptide interactions. However, due to the different coordination geometry of these metal ions differences may arise; in the case of the wild type prion protein fragments the metal binding preference was different; it shows a significant preference for Ni(II) binding at His96 residue (which is completely opposite to those reported for Cu(II) ion). It can be explained by the effect of the side chains, while nickel(II) ions form planar species where the shorter side chains are present, copper(II) ions are stabilized by axial interactions.

Smaller fragments of the tridecapeptide (Ac-PH^{85}AAA-NH_2 and Ac-$PH^{85}AAAGTH^{96}$S-NH_2) were also synthesized and studied for comparison.

2. Experimental

2.1. Chemicals

All solvents and chemicals used for synthesis were purchased from commercial sources in the highest available purity and used without further purification.

All N-fluorenylmethoxycarbonyl (Fmoc)-protected amino acids (Fmoc-Ala-OH, Fmoc-Gly-OH, Fmoc-His(Trt)-OH, Fmoc-Lys(Boc)-OH (Boc: tert-butyloxycarbonyl), Fmoc-Met-OH, Fmoc-Pro-OH, Fmoc-Ser (*t*Bu)-OH és Fmoc-Thr(*t*Bu)-OH), 2-(1-H-benzotriazole-1-yl)-1,1,3,3-tetramethyluronium tetrafluoroborate (TBTU) and Rink Amide AM resin was purchased from Novabiochem (Switzerland). *N*,*N*-diisopropyl-ethylamine (DIEA) and trifluoroacetic acid (TFA) were obtained from Merck Ltd. N-hydroxybenzotriazole (HOBt), *N*-methyl-pyrrolidone (NMP), triisopropylsilane (TIS), 2,2′-(ethylenedioxy)diethanethiol (DODT), and 2-methyl-2-butanol were Sigma-Aldrich products. Piperidine, dichloromethane (DCM), diethyl ether (Et_2O), acetic acid (96%) and H_2O_2 were obtained from Molar Chemicals Ltd., whereas peptide synthesis grade *N*,*N*-dimethylformamide (DMF), acetonitrile (ACN) and acetic anhydride were from VWR International Ltd. Ethylene diamine tetraacetic acid disodium salt (Na_2EDTA) were from Reanal Ltd.

The peptides Ac-PHAAAGTHSMKHM-NH_2, Ac-PHAAAGTHS-NH_2 and Ac-PHAAA-NH_2 were synthesized by means of a Liberty 1 solid phase peptide synthesizer.

Concentrations of the peptide stock solutions were determined by potentiometric titrations that also supported the purity and the identity of the substances.

Stock solutions of copper(II) chloride, copper(II) nitrate and nickel (II) chloride were prepared from analytical grade reagents and their concentration were measured gravimetrically via the precipitation of oxinates. The other stock solutions (KOH, HCl, KCl, potassium hydrogen phthalate) were also prepared from analytical grade reagents.

2.2. Peptide synthesis and purification

The protected peptides were synthesized by means of a microwave-assisted Liberty Peptide Synthesizer (CEM, Matthews, NC) using the Fmoc/tBu technique and the TBTU/HOBt/DIPEA (DIPEA: *N*,*N*-Diisopropylethylamine) activation strategy. Removal of the Fmoc protecting group was carried out at 80 °C with 30 W microwave power for 180 s by means of 20% piperidine in DMF. Four times excess of amino acids and 30 W microwave power for 300 s were used for coupling at 80 °C in the presence of 0.5 M HOBt and 0.5 M TBTU in DMF as an activator and 2 M DIPEA as an activator base. In the case of the peptides

the free amino terminus was treated with DMF containing 5 *V*/V% Ac_2O and 6 V/V% DIPEA to obtain the acetylated amino group. The prepared peptide linked to the resin was washed with dichloromethane, 96% acetic acid, 2-methyl-2-butanol and diethyl ether. The side chain protecting groups were cleaved with the mixture of TFA/TIS/H_2O/DODT (94/2.5/2.5/1 *V*/V%) at room temperature for 2 h. The solution containing the peptide was separated from the resin by filtration, followed by recovering from the pertinent solution by precipitation with cold diethyl ether. The precipitate was washed with cold diethyl ether, then was centrifuged and dried, redissolved in water and finally lyophilized.

The purity of the peptides was checked by analytical RP-HPLC using a Jasco instrument, equipped with a Jasco MD-2010 plus multi-wavelength detector. The chromatographic conditions are as follows: Column: Teknokroma Europa Protein C18 (250 × 4.6 mm, 300 Å pore size, 5 µm particle size); elution: gradient elution was carried out using solvent A (0.1% TFA in water) and solvent B (0.1% TFA in acetonitrile) at a flow rate of 1 mL·min^{-1}, monitoring the absorbance at 222 nm. From 0 min to 30 min 0% to 20% of ACN (Ac-PHAAAGTHSMKHM-NH_2), from 0 min to 30 min 0% to 12% of ACN (Ac-PHAAAGTHS-NH_2) A was applied (Scheme 2).

Ac-PHAAAGTHSMKHM-NH_2 was purified by the means of preparative HPLC equipped with semipreparative column (Vydac 218TP C18, 250 × 10 mm, 300 Å pore size, 5 µm particle size). Gradient elution was carried out using solvent A (0.1% TFA in water) and solvent B (0.1% TFA in acetonitrile) at a flow rate of 3 mL·min^{-1}, monitoring the absorbance at 222 nm. From 0 min to 30 min 95% to 85% then keeping this ratio for additional 10 min.

2.3. Potentiometric measurements

The pH-potentiometric titrations were made in 3.00 mL samples at 1–3·10^{-3} M ligand concentration with the metal ion to ligand ratios between 1:1 to 3:1 for the binary and 1:1:1 to the ternary system. The titrations were performed with carbonate free stock solution of potassium hydroxide of known concentration. A MOLSPIN pH-meter equipped with a 6.0234.100 combined glass electrode (Metrohm) was used for pH measurements (in the pH range 2.5–11.5), while the dosing of the titrant were made with a MOL-ACS microburette controlled by a computer.

During the measurements argon was bubbled through the samples to ensure the absence of oxygen and carbon dioxide. All pH-potentiometric measurements were carried out at a constant ionic strength of 0.2 M KCl and at a constant temperature (298 K).

The recorded pH readings were converted to hydrogen ion concentration as described by Irving et al. [32]. Protonation constants of the ligands and overall stability (log β_{pqr}) constants of the metal complexes were calculated by means of the general computational programs (SUPERQUAD [33] and PSEQUAD [34]) based on Eqs. (1) and (2).

$$pM + qH + rL = M_pH_qL_r \quad (1)$$

$$\beta_{pqr} = \frac{[M_pH_qL_r]}{[M]^p \cdot [H]^q \cdot [L]^r} \quad (2)$$

2.4. Spectroscopic measurements

UV–Vis spectra of the complexes were recorded on Hewlett Packard HP 8453 diode array and Perkin Elmer Lambda 25 double beam spectrophotometers. The same concentration range was used as for pH-potentiometry.

Circular dichroism spectra of the complexes were registered on a JASCO J-810 spectropolarimeter using 1 mm and/or cm cells in the 200–800 nm wavelength range at the same concentrations as used in pH-potentiometry.

2.5. Oxidation of the peptides

The reaction mixture containing 1.1 mM of peptides and metal-to-ligand molar ratio 1:1.1 was incubated at 25 °C for 1 h in the presence of hydrogen peroxide at metal to H_2O_2 molar ratio 1:4 for all peptides. The pH was adjusted to 7.4. The reaction was started by the addition of hydrogen peroxide, which was freshly prepared. After incubation the reaction was stopped by addition of Na_2EDTA at ligand to Na_2EDTA ratio 1:5. The reaction process was monitored by RP-HPLC at different time periods. The chromatograms of the reaction mixtures after 1 h 2, 4 and 24 and 96 h indicated no significant difference (the shape, retention times and intensity of peaks) suggesting the end of reaction after 1 h.

2.6. Isolation of oxidized products

The samples were analyzed by analytical RP-HPLC using a Jasco instrument, equipped with a Jasco MD-2010 plus multiwavelength detector. The oxidized products were conducted on a Teknokroma Europa Protein C18 (250 × 4.6 mm, 300 Å, 5 µm) at a flow rate of 1 mL·min^{-1}, monitoring the absorbance at 222 nm. Mobile phases were water (A) and acetonitrile (B) containing 0.1% TFA. Gradient: 0–3–9–24–30 min, 100–100–80–80–100% water containing 0.1% TFA for PGM; 0–3–9–24–30 min, 100–100–88–88–100% water containing 0.1% TFA for PG; 0–3–9–24–30 min.

2.7. Mass spectrometry

A maXis II MicroTOF-Q type Qq-TOF MS instrument (Bruker Daltonik, Bremen, Germany) was used for the MS and MS/MS measurements in positive ion mode. The instrument was equipped with an electrospray ion source where the spray voltage was 4 kV. N_2 was utilized as drying gas. The drying temperature was 200 °C and the flow rate was 4.0 L/min using the same method described in 2.6. For the MS/MS experiments, nitrogen was used as the collision gas. The pressure in the collision cell was determined to be 1.2 × 10^{-2} mbar. The precursor ions for MS/MS were selected with an isolation width of 5 *m/z* units. The mass spectra were recorded by means of a digitizer at a sampling rate of 2 GHz. The mass spectra were calibrated externally using the exact masses of clusters $[(Na\text{-formate})_n + Na]^+$ generated from the electrosprayed solution of sodium formate. The spectra were evaluated with the DataAnalysis 4.4 software from Bruker. The sample solutions were introduced either directly into the ESI source with a syringe pump (Cole-Parmer Ins. Co., Vernon Hills, IL, USA) at a flow rate of 3 µL/min.

3. Results and discussion

3.1. Protonation equilibria of the peptides

The protonation constants of the studied peptides and the stability constants of the corresponding copper(II) complexes were determined by means of potentiometric titrations and the data are reported in Table 1. The tridecapeptide contains a lysine and three histidine residues (see Scheme 1), while the penta- and nonapeptide contains only one and two histidine residues respectively. The protonation reactions of the side-chain imidazole moieties take place in a pH range of 5–8 in overlapping processes, while the highest pK value of Ac-PHAAAGTH-SMKHM-NH_2 can be unambiguously assigned to the deprotonation of the ε-ammonium group of the lysyl residue.

3.2. Copper(II) complexes of Ac-PHAAA-NH_2

This peptide mimics the complex formation properties of the octarepeat domain. The histidine residue is the anchor for coordination. The complex formation begins in the slightly acidic solution by the coordination of this group, which induces the deprotonation of amide nitrogens. However, because of the presence of proline, the amide

Table 1
pK values and stability constants of the copper(II) complexes of the studied peptides (I = 0.2 M KCl, T = 298 K, standard deviations are in parentheses).

	Ac-PHAAA-NH_2	Ac-PHAAAGTHS-NH_2	Ac-PHAAAGTHSMKHM-NH_2	Ac-$(PHGGGWGQ)_2$-NH_2 [14]	Ac-GTHSMKHM-NH_2 [17]
$pK(Im_1)$	6.43(1)	5.99(1)	5.59(3)	6.77	5.80
$pK(Im_2)$		6.75(1)	6.20(3)	6.97	6.61
$pK(Im_3)$			6.95(3)		
pK(Lys)			10.06(6)		10.19
CuH_2L			22.10(2)		
CuHL			16.89(2)	10.11	15.72
CuL		5.54(5)	9.88(8)	5.39	9.16
$CuH_{-1}L$		−1.03(9)	2.60(6)	–	2.67
$CuH_{-2}L$		−7.63(6)	−5.10(5)	−7.68	−5.50
$CuH_{-3}L$		−15.18(6)	−15.26(5)	−17.44	−15.78
$CuH_{-4}L$				−28.45	
$Cu_2H_{-1}L$			7.13(8)		
$Cu_2H_{-2}L$			1.26(2)		0.18
$Cu_2H_{-3}L$			−6.03(4)		−6.32
$Cu_2H_{-4}L$			−13.68(3)	−17.49	−14.00
$Cu_2H_{-5}L$			−22.14(3)	−26.55	−22.86
$Cu_2H_{-6}L$			−31.17(2)	−35.94	−33.43
$Cu_2H_{-7}L$				−46.42	
$Cu_2H_{-8}L$				−57.72	
$Cu_3H_{-3}L$			−1.89(12)		
$Cu_3H_{-4}L$			−8.45(13)		
$Cu_3H_{-5}L$			−15.27(9)		
$Cu_3H_{-6}L$			−23.23(13)		
$Cu_3H_{-7}L$			−31.70(10)		
$Cu_3H_{-8}L$			−42.59(28)		
$Cu_3H_{-9}L$			−52.96(10)		

deprotonation and coordination occurs towards the C-terminus forming 7-membered chelate ring (Scheme S1). The stability of this coordination mode is lower than the 6-membered one, and its formation is shifted to the higher pH values. As a consequence, the hydrolysis and the complex formation processes are in competition and precipitation occurs around pH 6. However, when the titration was performed from the basic solution towards the acidic one, the formation of precipitate was avoided. Stability constants were not determined, but several conclusions can be drawn from the UV–Vis and CD spectra. The spectra were taken originally basic solutions by the addition of acid. There are two well separated absorption maxima in the UV–Vis spectra (Fig. S1); at 520 nm and 630 nm. The first one is present in the strongly basic solution and typical for the 4N complexes. Its intensity decreases by decreasing pH until pH 10, than a red-shift of the absorption maximum occurs till 630 nm, which is characteristic for the 2N species; an amide nitrogen is coordinated in addition to the imidazole nitrogen. The low intensity band with an absorption maximum around 650–700 nm relates to the exclusive coordination of the imidazole nitrogen below pH 6.5. Similar conclusions can be drawn from the CD spectra (not shown). The $N^- \rightarrow Cu^{2+}$ charge transfer band around 305 nm confirms the presence of amide nitrogens in the coordination sphere of copper(II) ions.

3.3. Copper(II) complexes of Ac-PHAAAGTHS-NH_2

The complex formation reaction of this ligand with copper(II) ions were studied at different metal to ligand ratios. In the case of metal ion excess precipitation occurred, therefore stability constants were not determined for dinuclear species. However, this precipitate dissolved by pH 11, therefore certain consequences can be drawn.

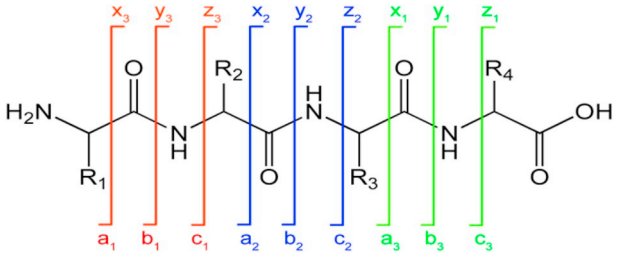

Scheme 2. Peptide fragmentation notation using the scheme of Roepstorff and Fohlman [35]

The complex formation begins around pH 4 by the formation of CuL. A low intensity band can be seen between 650 and 700 nm in the visible spectra. This can be explained by the formation of macrochelates with the exclusive coordination of imidazole nitrogens. This is also supported by the CD spectra because of the lack of any activity in this wavelength range.

The deprotonation of amide nitrogens occurs at higher pH. Species with 1, 2 or 3 coordinated amide nitrogens are also present. Due to the two histidine residues, isomer structures can be formed. If the amide coordination begins from the histidine at the eight position towards the N-terminus six-membered chelate forms, while in the other case this process occurs with histidine at the second position towards the C-terminus resulting seven-membered chelate.

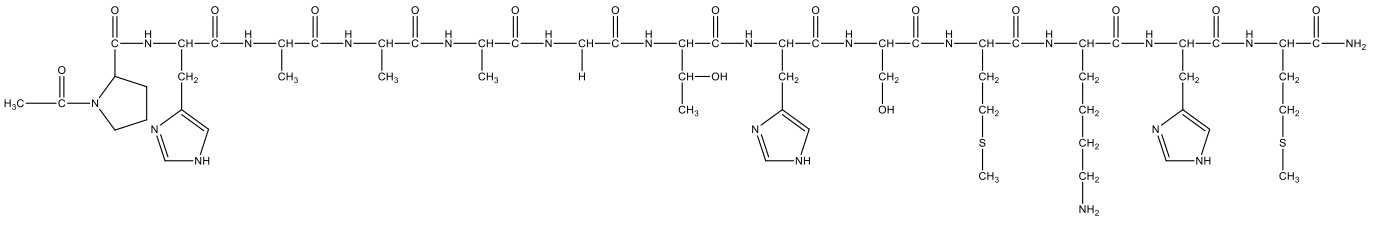

Scheme 1. Structure of the studied Ac-PHAAAGTHSMKHM-NH_2 peptide

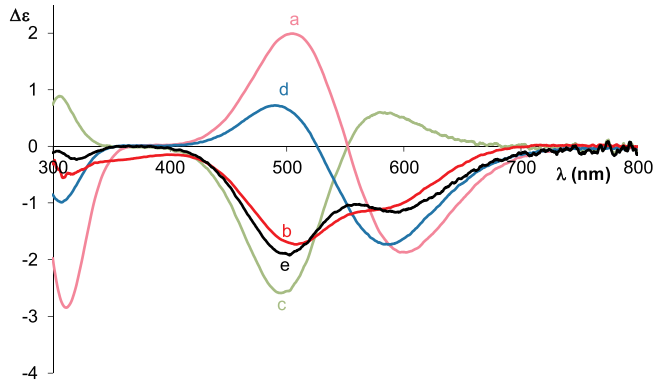

Fig. 1. CD spectra of the Cu(II): Ac-PHAAAGTHS-NH_2 system at 1:1 (a) and 2:1 (b) metal to ligand ratio, the Cu(II):Ac-PHAAA-NH_2 (c) and Cu(II):Ac-GTHS-NH_2 systems at 1:1 ratio (d) at pH 11, and the sum of the CD spectra of the Cu (II):Ac-PHAAA-NH_2 = 1:1 and the Cu(II):Ac-GTHS-NH_2 = 1:1 systems (e).

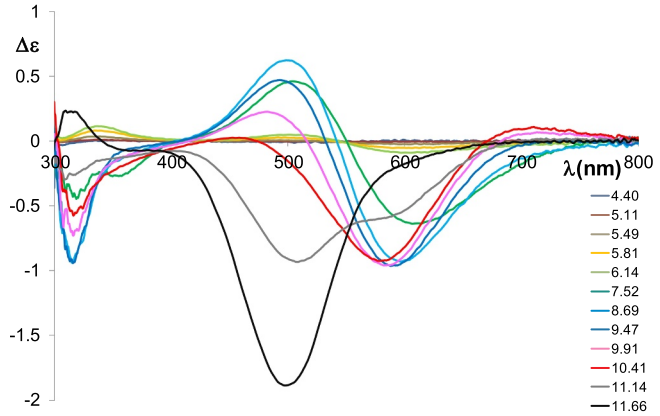

Fig. 2. CD spectra of the Cu(II):Ac-PHAAAGTHS-NH_2 system at 2:1 metal to ligand ratio at different pH values ($c_L = 3{\cdot}10^{-3}$ M).

It is proved by the comparison of the CD spectra of the His85 and His96 model peptides (Fig. 1), that the first equivalent of copper(II) coordinates to the binding site outside the octarepeat domain. However, the one magnitude order higher stability constant proposes the axial coordination of the other histidine side chain. On the other hand, above 8.5 this peptide is able the bind two equivalent of copper(II) ions. It is also proved by the CD spectra (Fig. 2). The CD activity is increasing until this pH; there is a positive and a negative Cotton effect around 500 and 600 nm, respectively. If the pH is further increased the intensity of the CD band is decreasing drastically around 500 nm, which will be turned to negative Cotton effect by pH 11. The negative Cotton effect can be seen also at this pH around 600 nm in the envelope curve, but disappears at higher pH. It turned out by the comparison of the CD spectra that below pH 11, one copper(II) ion is bounded to the PHAAA-, and the other one is bounded to the -GTHS domain forming (7,5,5) and (6,5,5) chelates, respectively with the same (N(Im),N^-,N^-,N^-) donor atoms. Above pH 11 the CD spectrum is in good agreement with the spectra of common tetrapeptide complexes. According to this it is suggested, that the histidine residue of the octarepeat part is displaced by a fourth amide nitrogen and a (5,5,5)-membered fused chelate forms.

3.4. Copper(II) complexes of Ac-PHAAAGTHSMKHM-NH_2

The Ac-PHAAAGTHSMKHM-NH_2 tridecapeptide contains three histidine residues mimicking three metal binding sites from three different regions of the prion protein. As it was expected this ligand can bind three equivalents of Cu(II) ions, the stability constants of the

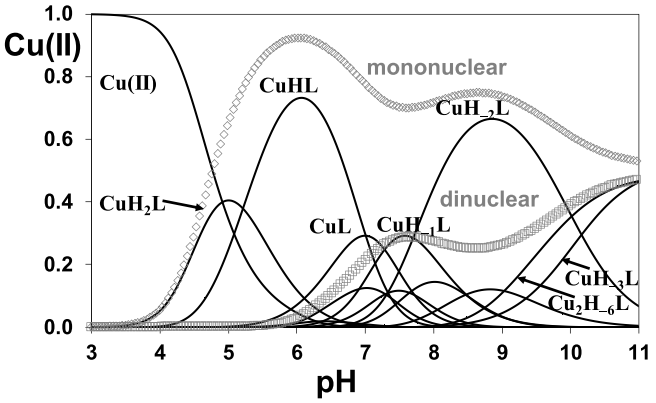

Fig. 3. Metal ion speciation of the copper(II)-Ac-PHAAAGTHSMKHM-NH_2 system in equimolar solution ($c_{Cu(II)} = c_L = 1$ mM).

peptides are summarized in Table 1, whereas the corresponding speciation curves are shown on Fig. 3 and S2. There is a low intensity absorption band in the pH range 4–6, and its maximum is around 650–700 nm, which refers to the exclusive coordination of the imidazole nitrogens. It is also supported by the lack of CD activity in this pH range. In addition to the lysine side chain, one of the imidazole nitrogens is also protonated in the CuH_2L species, and the other two imidazole nitrogens are coordinated to the copper(II) ion. The formation of the singly protonated CuHL species is almost parallel with CuH_2L. Its logK(Cu(II) + N_{Im}) value is 6.83, which is between the value of complexes with the coordination of two and three imidazole nitrogens. This data proves the presence of macrochelates in which two or three imidazole nitrogens are coordinated in this pH range. The further increase of the pH values results in a continuous blue shift of the absorption spectra and the appearance of the $N^- \rightarrow Cu^{2+}$ CT band (λ_{max} = 310 nm) in the CD spectra. These processes are due to the deprotonation of the amide nitrogens and the formation of the 2 N CuL, 3 N $CuH_{-1}L$ and 4 N $CuH_{-2}L$ species. The latter species has high stability and dominant in the pH range 8–10. There is no other change in the spectra above pH 10, since the last deprotonation process is owing to the deprotonation of the ε-ammonium group of lysine side chain.

The amount of dinuclear complexes is considerable even in equimolar solution. The statistical probability of the formation of dinuclear species in the case of three binding sites and one metal ion is 44% [11]. The amount of dinuclear species is slightly lower than the statistical value; 30% in the physiological pH-range, that leads us to conclude that the three binding sites are not equivalent. However, this value reaches the statistical data above pH 10.

The intensities of the CD spectra (Fig. 4) are rather low, and in the case of 1:1 and 2:1 copper(II) to ligand ratios, their exteriors are similar

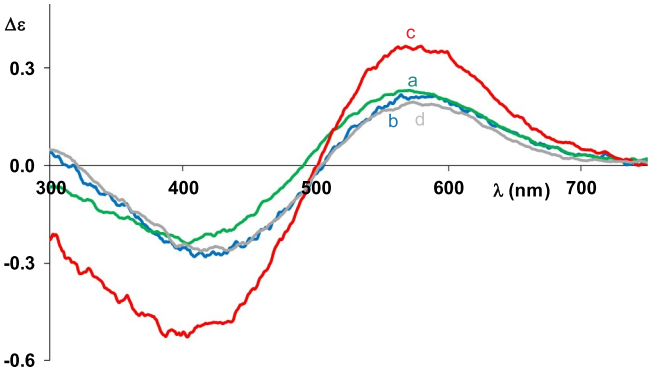

Fig. 4. CD spectra of the Cu(II):Ac-PHAAAGTHSMKHM-NH_2 system at 1:1 (a), 2:1 (b) and 3:1 (c) metal to ligand ratio and CD spectrum of the Cu (II):Ac-GTHSMKHM-NH_2 at 1:1 metal to ligand ratio (d) around pH 8.

Table 2
Stability constants of the nickel(II) complexes of Ac-PHAAAGTHSMKHM-NH_2 (I = 0.2 M KCl, T = 298 K, standard deviations are in parentheses).

	Ac-PHAAAGTHSMKHM-NH_2	Ac-GTHSMKHM–NH_2 [19]	Ac-GTHS-NH_2 [36]	Ac-MKHM-NH_2 [36]
NiHL	14.19(2)	13.71		13.09
NiL	5.83(8)		2.82	5.08
$NiH_{-2}L$	−11.12(5)	−10.92		
$NiH_{-3}L$	−20.95(6)	−20.62		
$Ni_2H_{-2}L$	−7.31(5)	−7.99		
$Ni_2H_{-4}L$	−24.48(5)			
$Ni_2H_{-5}L$	−33.36(4)	−33.22		
$Ni_2H_{-6}L$	−43.73(6)	−43.59		

to the $Cu_2H_{-6}L$ species of Ac-GTHSMKHM-NH_2 which also can be calculated by a simple superposition of the spectra of $CuH_{-3}L$ of the His96 and His111 model peptides. It means that the first two equivalents of copper(II) ion coordinate to the sequence mimicking histidines outside the octarepeat domain (-GTHS- and -MKHM-) in comparable concentration. However, in the case of 3:1 copper(II) to ligand ratio the increase of the negative Cotton effect below 500 nm refers to the coordination of the imidazole nitrogen of the octarepeat part of the peptide. It means that the metal binding affinity of histidine mimicking the octarepeat domain is decreased, preference for the binding sites follows the order His111 ~ His96 > His85.

3.5. Nickel(II) complexes of Ac-PHAAAGTHSMKHM-NH_2

The complex formation processes of this ligand was also studied by nickel(II) ions. The stability constants of the formed nickel(II) complexes and these data of the peptides used for comparison are collected in Table 2. It was found that this peptide is not able to bind as many nickel(II) ions as the number of independent histidyl residues in the sequence; only mono and dinuclear species are present in the solution. The species NiHL predominates at 1:1 and 2:1 metal to ligand ratios between pH 6 and 8. The lack of CD activity suggests octahedral geometry, where macrochelate forms by the coordination of imidazole nitrogens. Its relatively high stability ($logK(NiH_{-1}L) + N_{Im}$) = 4.13) supports the coordination of more than two imidazole nitrogens. This value was 3.52 in the case of Ac-GTHSMKHM-NH_2, where the coordination of two imidazole nitrogens is possible. There is an extra base consuming process above pH 8, which is accompanied by the appearance of the intensive square planar band in the UV–Vis spectra. The stoichiometry of the first amide coordinated complex is NiL, in which the lysine side chain is protonated, therefore its exact formula is $(NiH_{-1}L)H$. The deprotonation of the amide nitrogens is not fully cooperative because of the presence and the coordination of the three imidazole nitrogens. The stoichiometry of the main species formed in the pH range 8.8–10.0 is $NiH_{-2}L$ ($(NiH_{-3}L)H$), where the absorption maxima do not change, only the intensity is increasing. (5,5,6)-membered chelate rings are formed, with ($3N^-$,N_{Im}) coordination modes. The formation of $[NiH_{-3}L]$ species is not accompanied by any spectral change, since it is due to the deprotonation of the ε-amino group of the lysine residue. In addition to the above-mentioned species, dinuclear complexes are also formed even in the equimolar samples. The ratio of this species is approximately 20%. On the other hand they are the exclusive species at 2:1 nickel to ligand ratio in the pH range where the deprotonation of amide nitrogens occurs. There is possibility for the formation of coordination isomers due to the presence of the three histidine residues. Information about the ratio of these isomers can be obtained from the CD spectra. Fig. S3 presents the effect of increasing concentration of nickel ions on the CD spectra at pH 10.5. The shape and the intensity of the spectrum at 1:1 ratio is similar to the Ni(II)-Ac-GTHS-NH_2 system. This points to the fact that the first equivalent nickel ion binds to the -GTHS- part of the peptide which represents the His96 domain of the human prion protein. The intensity is decreasing by the increasing amount of nickel ion, which can be explained by the coordination of nickel ion to the -MKHM- part with reversed CD activity.

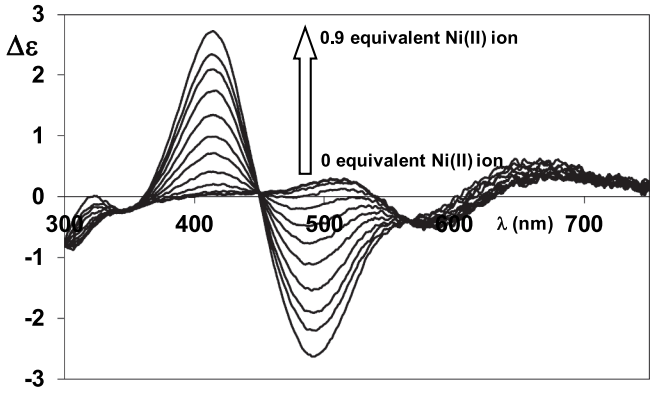

Fig. 5. Effect of the addition of Ni(II) ions on the CD spectra of the Cu(II):Ac-PHAAAGTHSMKHM-NH_2 = 1:1 system around pH 10.5.

3.6. Copper(II)-nickel(II) mixed metal complexes of Ac-PHAAAGTHSMKHM-NH_2

Since the peptide is able to bind three equivalents of Cu(II) ions or two equivalents of Ni(II) ions, the Cu(II):Ni(II):L = 1:1:1 system was also studied. Due to the formation of precipitate around pH 8, stability constants were not determined. However, it dissolved by increasing pH, therefore spectroscopic measurements were carried out. Fig. 5 shows the change of CD spectra of the equimolar Cu(II):L = 1:1 system at pH 10.5 by the addition of nickel(II) ions. In the initial solution copper (II) ions are coordinated in comparable concentration to the sequences mimicking histidines from outside the octarepeat domain (-GTHS- and -MKHM-). Continuously increasing CD activity can be seen by the addition of nickel ions. The nickel ions are not able to remove copper(II) ions, only redistribute between the available binding sites; copper(II) will bind mainly to -MKHM-, while nickel(II) will bind to the -GTHS- sequence. The distribution of the metal ions can be seen on Fig. 6.

3.7. Copper(II) catalyzed oxidation of Ac-PHAAAGTHS-NH_2

Ac-PHAAAGTHS-NH_2 peptide was oxidized with the Cu(II):L:H_2O_2 = 1:1:4 system around pH 7.4 where the 3 N and 4 N species are present in approximately 1:1 ratio.

An oxidized product containing an additional oxygen atom and peptide fragments are also formed during the oxidation. Scheme 2 presents the peptide fragmentation notation for a tetrapetide. Peptide fragment ions are indicated by a, b, or c if the charge is retained on the N-terminus and by x, y or z if the charge is maintained on the C-terminus. The subscript indicates the number of amino acid residues in the fragment [35].

Three main products are identified in the HPLC chromatogram; the ligand with an additional oxygen atom (y_9 + O) and two fragments of it; the N-terminal fragment containing six amino acid residues (c_6) and the oxidized form of the C-terminal fragment (z_3 + O).

The MS/MS spectrum of the oxidized product of Ac-PHAAAGTHS-NH_2 ($[y_9 + O]^{2+}$ ion) is shown on Fig. 7. It is fragmented into c_6^+ and $[z_3 + O]^+$ ions. The identity of these ions was proved also by fragmentation, which is presented on Figs. 8 and 9. During the fragmentation of the ion c_6^+ the first step is the formation of b_6^+ by the loss of NH_3. Then not only the series of b^+ ions, but also a_2^+-a_5^+ ions were identified. The fragmentation of b_6^+ and a_5^+ ion begins on the C-terminus, and the amino acids are removed step by step.

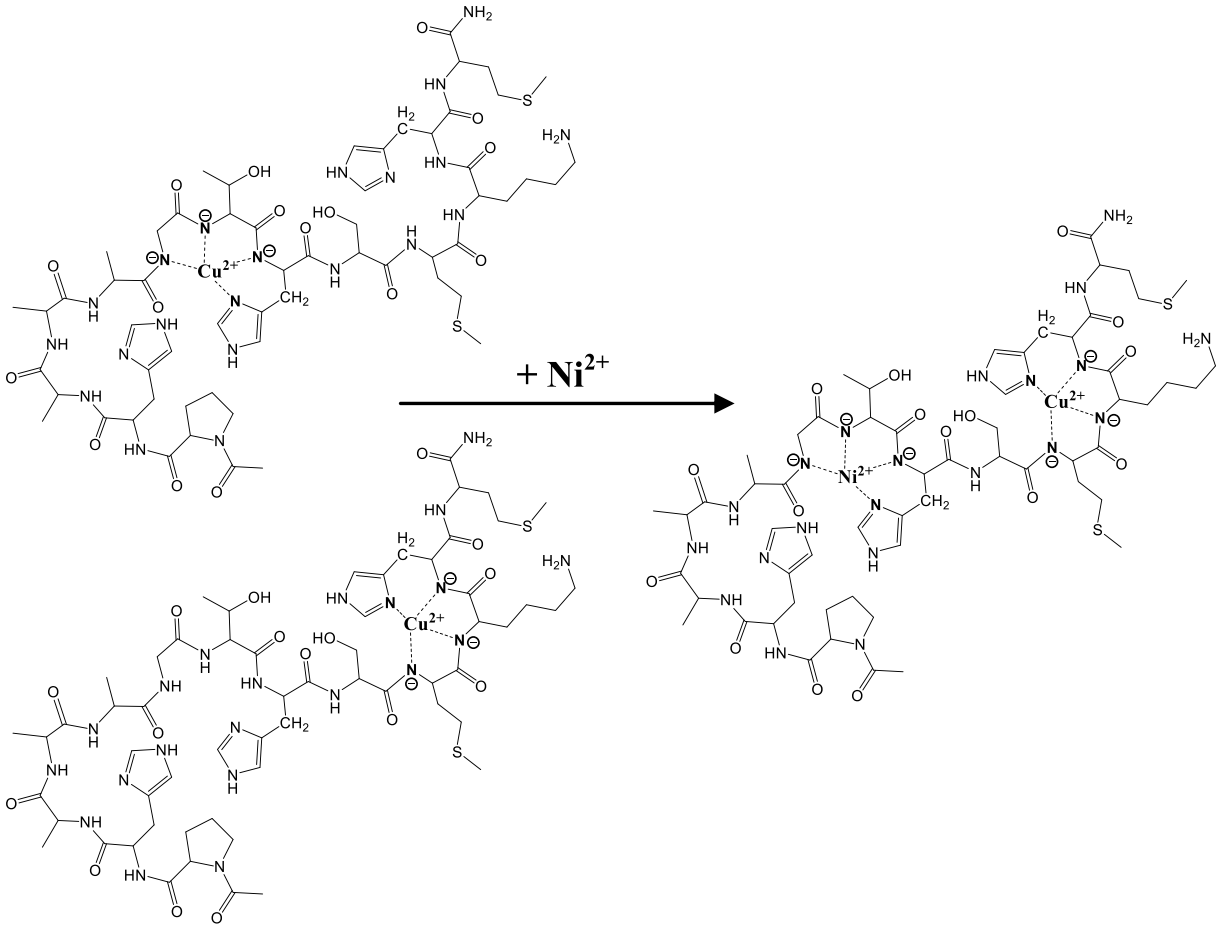

Fig. 6. Coordination isomers of the 4N coordinated species formed in the Cu(II):Ac-PHAAAGTHSMKHM-NH_2 = 1:1 system and the supposed structure of the mixed metal complex formed in the Ni(II):Cu(II):Ac-PHAAAGTHSMKHM-NH_2 = 1:1:1 system.

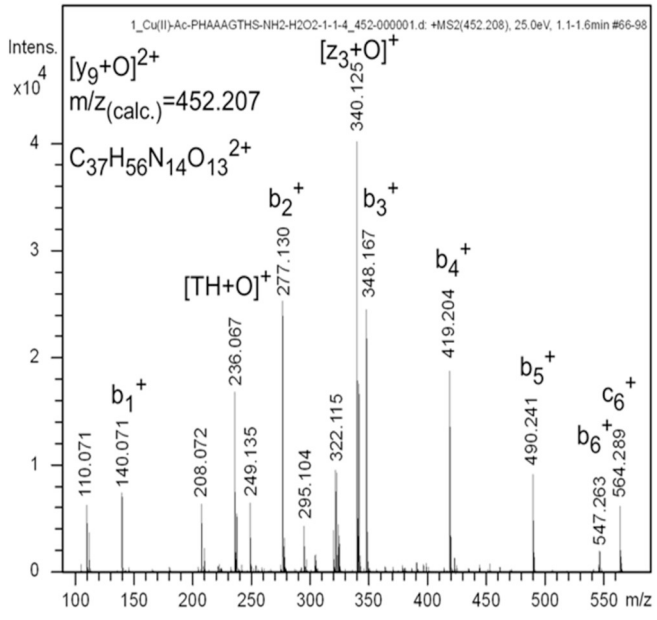

Fig. 7. MS/MS spectrum of the $[y_9 + O]^{2+}$ ion formed during the oxidation of Ac-PHAAAGTHS-NH_2.

The fragmentation pattern of $[z_3 + O + 2H]^+$ ion is used for finding the localization of oxidation. The first step is the loss of a H_2O molecule and the formation of an ion with 324.130 *m/z*, then an ion with 324.130 *m/z* is formed by the loss of an NH_3 molecule. However, the oxidation of histidine is proved by the loss of CH_3NO (45.011 *m/z*). The presence of the internal $[TH + O]^+$ ion also supports the formation of 2-oxo-histidine. This ion loses a CO molecule, then the cleavage of the oxidized imidazole ring occurs by the loss of $C_2H_2N_2O$ group (60.016 *m/z*).

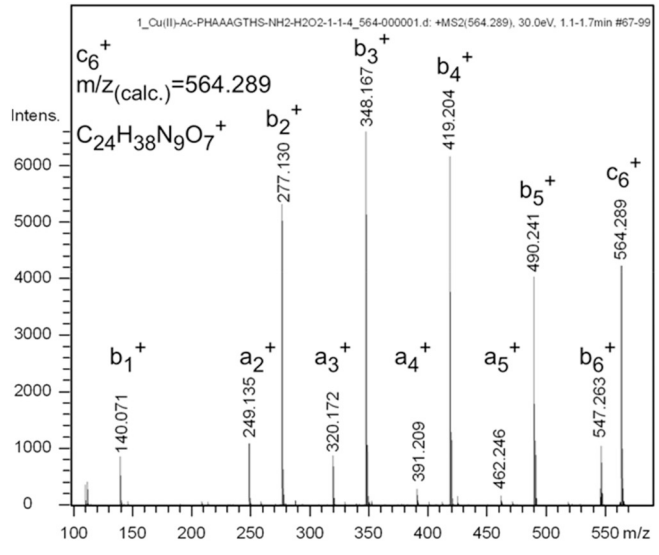

Fig. 8. MS/MS spectrum of the $[c_6]^+$ ion formed during the oxidation of Ac-PHAAAGTHS-NH_2.

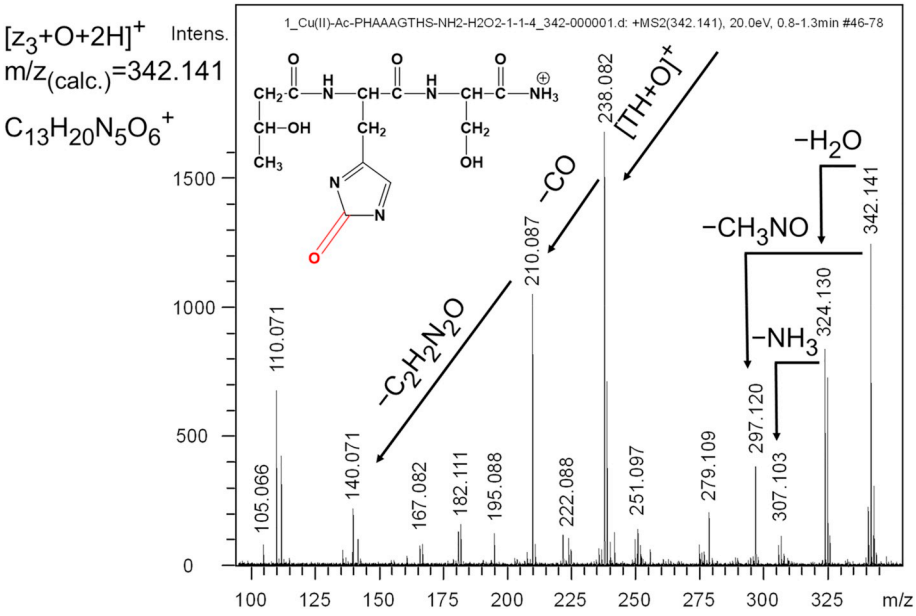

Fig. 9. MS/MS spectrum of the $[z_3 + O + 2H]^+$ ion formed during the oxidation of Ac-PHAAAGTHS-NH_2.

3.8. Copper(II) catalyzed oxidation of Ac-PHAAAGTHSMKHM-NH_2

The Ac-PHAAAGTHSMKHM-NH_2 peptide was oxidized by the Cu(II):L:H_2O_2 = 1:1:4 system. The oxidation of this peptide is excessively complicated. There are five amino acids namely three histidine and two methionine residues which are involved in the oxidation, and the addition of two oxygen atoms on the same side chain is also possible. The formation of fragments containing 1–5 additional oxygen atoms and the fragmentation of the Gly(6)-Thr(7) peptide bonds also occurs in this system. However, the chance for the multiple oxidation of peptides is very low in biological systems, therefore we will focus on the discussion of the singly oxidized products.

The most intensive peaks in the MS/MS spectra of $[y_{10} + O]^+$ (Fig. 10) arise from the fragmentation of the b_6^+ ion with 547.262 *m/z* (calculated value 547.262), according to it, the oxidation of the His2(His^{85}) residue does not occur in this case. However, the oxidation of His8 (His^{96}) is proved by the internal $[His8(O)S\text{-}H_2O]^+$ species with 223.080 *m/z* (calculated value 223.083), while there is no direct proof for the oxidation of His12(His^{111}), it may also occur, but in smaller extent. On the other hand, on the base of the highly oxidized products the oxidation of every histidine residue may occur, even the addition of two oxygen atoms on the same site is also possible. There are several proofs for the doubly oxidation of histidine residues. For example in the fragment $[c_9 + 3O]^+$ three additional oxygen atoms are bound, although it contains only two histidine residues. Hence, one of these histidine residues is doubly oxidized. Therewith the loss of a CH_3NO group supports the oxidation of a histidine residue, while the loss of a $CHNO_2$ group supports the doubly oxidation of it.

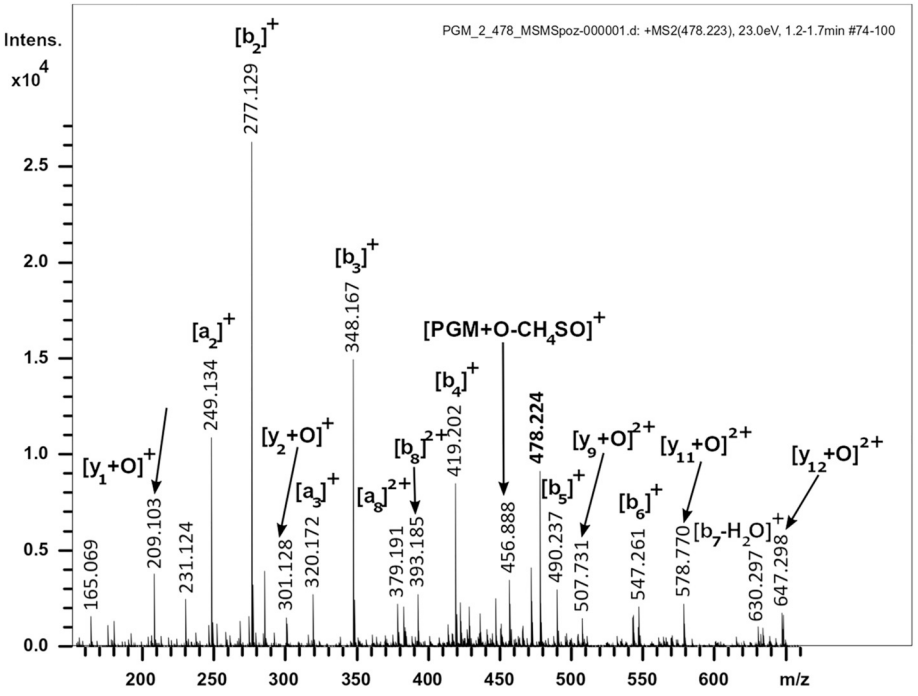

Fig. 10. MS/MS spectrum of the singly oxidized product of Ac-PHAAAGTHSMKHM-NH_2.

The order of tendency for oxidation is His96 > His85 ≫ His111. However in the case of the singly oxidized products, only the oxidation of His96 residue is proved. The difference in the copper(II) ion oxidation susceptibility may be due to the steric arrangement of the peptide. The copper(II) ion is easily available for the hydrogen peroxide in the case of the -GTHS- domain, where the side chains are relatively small. However, owing to the axial interactions of the larger side chains in the -MKHM- domain the copper(II) ion is locked and therefore the oxidation at that position occurs to a smaller extent.

The oxidation of the two methionine residues cannot be avoided. For example the $[y_1 + O]^+$ ion with 165.068 *m/z* (calculated value 165.069) supports the oxidation of Met13 (Met^{112}), while in the case of the fragmentation of the quadruply oxidized peptide the $[y_2 + O\text{-}CH_3SOH]^+$ ion with 238.127 *m/z* (calculated value 238.130) supports the oxidation of Met10 (Met^{109}), and the presence of TH(O)SM(O) with 617.266 *m/z* (calculated value 617.271) confirms the oxidation of both His8 (His^{85}) and Met10 (Met^{109}) residues.

4. Conclusions

Previous studies on the copper(II) and nickel(II) complexes of peptide fragments of prion protein indicated a different binding preference for the metal ion coordination at the various histidyl sites. In the case of the histidine residues outside the octarepeat region His96 > His111 was reported for nickel(II) and the opposite trend for copper(II), while the histidine residue in the octarepeat region has smaller metal binding ability with both metal ions. However, in the case of Ac-GTHSMKHM-NH_2 the binding sites which are outside the octarepeat region are equivalent for copper(II), while His96 is preferred for nickel (II). The same consequence can be drawn in the case of the presently studied Ac-PHAAAGTHSMKHM-NH_2 tridecapeptide. The tridecapeptide is able to bind three equivalent of copper(II) ions, since the histidine residues behave as independent metal binding sites. Nevertheless the metal binding ability of histidine residue mimicking the octarepeat domain (His85) is decreased, while the other parts of the peptide mimicking the histidine residues outside the octarepeat domain binds the copper(II) ions in comparable concentration. On the other hand, this peptide is able to coordinate only two equivalents of nickel ion on the domains outside the octarepeat region, furthermore the His96 binding site is more effective for the nickel ions. It is also supported by the formation of mixed metal complexes, where the nickel(II) ions bind the -GTHS- domain, the copper(II) ions are displaced from there and occupy the -MKHM- domain. The lower metal binding ability of the histidine in the octarepeat region is confirmed by the shorter fragments. The metal binding of the His85 residue in the case of these fragments is accompanied by precipitation.

The order of copper(II) binding affinity of the various histidyl sites is His111 ~ His96 > His85, while the order of oxidation activity is His96 > His85 ≫ His111. The metal binding ability of the histidine residues outside the octarepeat region is almost comparable, but the susceptibility for oxidation differs. The first order can be explained by the fact that the coordination mode at the -GTHS- and -MKHM- domain is the same, (N_{im},N^-,N^-) in the form of (6,5,5)-membered fused chelate rings, which is preferred over the (7,5,5)-membered one.

Declaration of competing interest

The authors declare that they have no known competing financial interests or personal relationships that could have appeared to influence the work reported in this paper.

Acknowledgments

The authors thank the Hungarian Scientific Research Fund (NKFI-115480 and NKFI-124983) for its financial support. The research was supported by the EU and co-financed by the European Regional Development Fund under the project GINOP-2.3.2-15-2016-00008. The research was also supported by the János Bolyai Research Scholarship of the Hungarian Academy of Sciences.

Appendix A. Supplementary data

Supplementary data to this article can be found online at https://doi.org/10.1016/j.jinorgbio.2019.110927.

References

[1] D.C. Bolton, M.P. McKinley, S.B. Prusiner, Science 218 (1982) 1309–1311.
[2] R. Riek, S. Hornemann, G. Wider, M. Billeter, R. Glockshuber, K. Wüthrich, Nature (London) 382 (1996) 180–182.
[3] A. Aguzzi, M. Heikenwalder, M. Polymenidou, Nat. Rev. Mol. Cell Biol. 8 (2007) 552–561.
[4] S.B. Prusiner, Brain Pathol. 8 (1998) 499–513.
[5] S.B. Prusiner, Proc. Natl. Acad. Sci. U. S. A. 95 (1998) 13363–13383.
[6] K.-M. Pan, M. Baldwin, J. Nguyen, M. Gasset, A. Serban, D. Groth, I. Mehlhorn, Z. Huang, R.J. Fletterick, F.E. Cohen, S.B. Prusiner, Proc. Natl. Acad. Sci. U. S. A. 90 (1993) 10962–10966.
[7] L. Gasperini, E. Meneghetti, B. Pastore, F. Benetti, G. Legname, Antioxid. Redox Signal. 22 (2015) 772–784.
[8] X.T.A. Nguyen, T.H. Tran, D. Cojoc, G. Legname, Mol. Neurobiol. 56 (2019) 6121–6133.
[9] G. Arena, D. La Mendola, G. Pappalardo, I. Sóvágó, E. Rizzarelli, Coord. Chem. Rev. 256 (2012) 2202–2218.
[10] G. Di Natale, G. Grasso, G. Impellizzeri, D. La Mendola, G. Micera, N. Mihala, Z. Nagy, K. Osz, G. Pappalardo, V. Rigó, E. Rizzarelli, D. Sanna, I. Sóvágó, Inorg. Chem. 44 (2005) 7214–7225.
[11] K. Ősz, Z. Nagy, G. Pappalardo, G. Di Natale, D. Sanna, G. Micera, E. Rizzarelli, I. Sóvágó, Chem. Eur. J. 13 (2007) 7129–7143.
[12] G. Di Natale, K. Ősz, Z. Nagy, D. Sanna, G. Micera, G. Pappalardo, I. Sóvágó, E. Rizzarelli, Inorg. Chem. 48 (2009) 4239–4250.
[13] H. Kozlowski, W. Bal, M. Dyba, T. Kowalik-Jankowska, Coord. Chem. Rev. 184 (1999) 319–346.
[14] C.S. Burns, E. Aronoff-Spencer, C.M. Dunham, P. Lario, N.I. Avdievich, W.E. Antholine, M.M. Olmstead, A. Vrielink, G.J. Gerfen, J. Peisach, W.G. Scott, G.L. Millhauser, Biochem 41 (2002) 3991–4001.
[15] D. Valensin, M. Luczkowski, F.M. Mancini, A. Legowska, E. Gaggelli, G. Valensin, K. Rolka, H. Kozlowski, Dalton Trans. (2004) 1284–1293.
[16] G. Di Natale, K. Ősz, C. Kállay, G. Pappalardo, D. Sanna, G. Impellizzeri, I. Sóvágó, E. Rizzarelli, Chem. Eur. J. 19 (2013) 3751–3761.
[17] C.E. Jones, S.R. Abdelraheim, D.R. Brown, J.H. Viles, J. Biol. Chem. 279 (2004) 32018–32027.
[18] I. Turi, C. Kállay, D. Szikszai, G. Pappalardo, G. Di Natale, P. De Bona, E. Rizzarelli, I. Sóvágó, J. Inorg. Biochem. 104 (2010) 885–891.
[19] I. Turi, D. Sanna, E. Garribba, G. Pappalardo, I. Sóvágó, Polyhedron 62 (2013) 7–17.
[20] B.S. Berlett, E.R. Stadtman, J. Biol. Chem. 272 (1997) 20313–20316.
[21] D.A. Butterfield, J. Kanski, Mech. Ageing Dev. 122 (2001) 945–962.
[22] J.D. Bridgewater, R.W. Vachet, Anal. Biochem. 341 (2005) 122–130.
[23] T. Kowalik-Jankowska, M. Ruta, K. Wiśniewska, L. Łankiewicz, M. Dyba, J. Inorg. Biochem. 98 (2004) 940–950.
[24] F. Zhao, E. Ghezzo-Schoneich, G.I. Aced, J. Hong, T. Milby, C. Schoneich, J. Biol. Chem. 272 (1997) 9019–9029.
[25] S. Li, T.H. Nguyen, C. Schoneich, R.T. Borchardt, Biochem 34 (1995) 5762–5772.
[26] A. Amici, R.L. Levine, L. Tsai, E.R. Stadtman, J. Biol. Chem. 264 (1989) 3341–3346.
[27] E.R. Stadtman, Free Radic. Biol. Med. 9 (1990) 315–325.
[28] C.C. Chao, Y.S. Ma, E.R. Stadtman, Proc. Natl. Acad. Sci. U. S. A. 94 (1997) 2969–2974.
[29] M.L. McKee, J. Am. Chem. Soc. 120 (1998) 3963–3969.
[30] F. Jensen, A. Greer, E.L. Clennan, J. Am. Chem. Soc. 120 (1998) 4439–4449.
[31] G. Csire, L. Nagy, K. Várnagy, C. Kállay, J. Inorg. Biochem. 170 (2017) 195–201.
[32] H. Irving, G. Miles, L.D. Pettit, Anal. Chim. Acta 38 (1967) 475–488.
[33] L. Zékány, I. Nagypál, D.J. Leggett (Ed.), Computational Methods for the Determination of Stability Constants, Plenum Press, New York, 1985.
[34] P. Gans, A. Sabatini, A. Vacca, J. Chem. Soc. Dalton Trans. (1985) 1195–1200.
[35] P. Roepstorff, J. Fohlman, Biomed. Mass Spectrom. 11 (11) (1984) 601–610.
[36] V. Jószai, Z. Nagy, K. Ősz, D. Sanna, G. Di Natale, D. La Mendola, G. Pappalardo, E. Rizzarelli, I. Sóvágó, J. Inorg. Biochem. 100 (2006) 1399–1409.